MULTIDIMENSIONAL NONSUBSAMPLED HOURGLASS FILTER BANKS: GEOMETRY OF PASSBAND SUPPORT AND FILTER DESIGN

Yue Lu and Minh N. Do

Department of Electrical and Computer Engineering
University of Illinois at Urbana-Champaign, Urbana, IL 61801, USA
Email: {yuelu, minhdo}@uiuc.edu; Web: www.ifp.uiuc.edu/∼{yuelu, minhdo}

ABSTRACT

Recently, the classical two-dimensional directional filter banks have been extended to higher dimensions. In this paper, we study one of the key components in this new construction, namely the multidimensional nonsubsampled hourglass filter banks. Starting with a rigorous analysis on the geometry of multidimensional hourglass-shaped passband supports, we propose a novel design for these filter banks in arbitrary dimensions, featuring perfect reconstruction and finite impulse response (FIR) filters. We analyze necessary and sufficient conditions for the resulting filters to achieve good frequency responses, and provide an optimal solution that satisfies these conditions using simplest filters. The proposed filter design technique is verified by a design example in 3-D.

1. INTRODUCTION

Recently, the classical two-dimensional (2-D) directional filter banks (DFB) [1] have been extended to higher dimensions [2]. As shown in Figure 1, the passband supports of the new filter banks (named NDFB) in 3-D are rectangular-based pyramids, radiating out from the origin at different orientations and tiling the entire frequency space. In general, the NDFB can decompose a d-D ($d \geq 2$) signal into directional subbands with hyperpyramid-shaped supports.

Multidimensional filters with similar directional passbands have been previously proposed in the literature [3, 4], and are shown to be useful in a wide range of applications, including video processing, seismic imaging, computer graphics, medical image analysis, and many others.

In this paper, we focus on one of the key components in NDFB, namely the multidimensional nonsubsampled *hourglass filter banks*. This name comes from the fact that these filter banks have an hourglass-shaped frequency partitioning, as shown in Figure 2 for the 2-D case and in Figure 3 for the 3-D case. We can see from Figure 3 that, unlike traditional critically-sampled filter banks, the hourglass filter banks discussed in this paper are nonsubsampled, i.e., without downsampling or upsampling operations. Despite the redundancy (a factor of d for the d-D case) in the filter banks, we can show [2] that this nonsubsampled construction is crucial in simplifying subsequent levels of decompositions in NDFB.

This work was supported by the US National Science Foundation under Grant CCR-0237633 (CAREER).

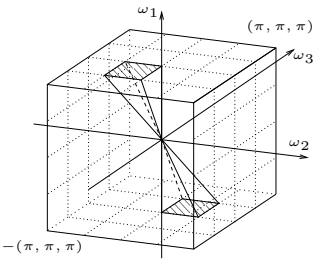

Fig. 1. Frequency partitioning of NDFB in 3-D.

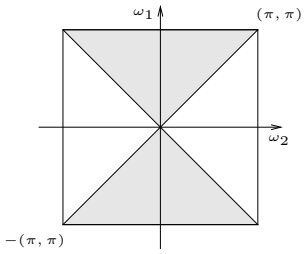

Fig. 2. 2-D hourglass filters.

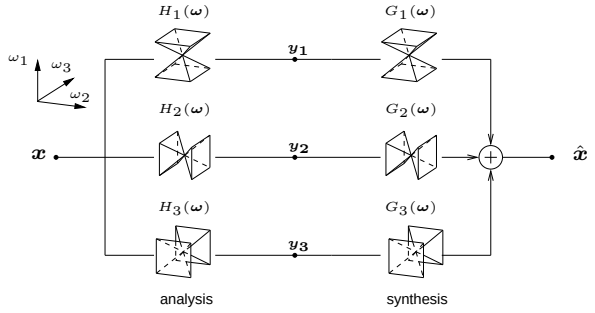

Fig. 3. The nonsubsampled hourglass filter bank in 3-D.

The hourglass filter banks in 2-D have been extensively studied in the past [5]–[8]. However, to our best knowledge, studies on hourglass filter banks in 3-D and higher dimensions have not been previously reported. In this work, we provide a rigorous analysis on the geometry of multidimensional hourglass-shaped passband supports. Meanwhile, we propose a novel design for these filter banks in arbitrary dimensions, featuring perfect reconstruction and finite impulse response (FIR) filters.

The rest of the paper is organized as follows. In Section 2, we have a formal definition of the passband supports of multidimensional hourglass filter banks. We describe our filter bank design technique in Section 3 and show numerical examples in Section 4.

2. GEOMETRY OF MULTI-DIMENSIONAL HOURGLASS FILTERS

2.1. Preliminaries

Throughout the paper, d represents the dimension of the filters under consideration. We are interested in cases when $d \geq 2$. We use lower-case letters, such as $x[\boldsymbol{n}]$, to denote a d-D discrete filter, where $\boldsymbol{n} = (n_1, n_2, \ldots, n_d)^T$ is an integer vector. Let $\boldsymbol{\omega} = (\omega_1, \ldots, \omega_d)^T$, and the frequency response $X(e^{j\boldsymbol{\omega}})$ of the filter is given by

$$X(e^{j\boldsymbol{\omega}}) = \sum_{\boldsymbol{n}\in\mathbb{Z}^d} x[\boldsymbol{n}]e^{-j\boldsymbol{\omega}^T\boldsymbol{n}}.$$

Ideally, the frequency response $X(e^{j\boldsymbol{\omega}})$ is an indicator function $I_{\mathcal{X}}(\boldsymbol{\omega})$ on its idealized passband support $\mathcal{X}$. In reality however, the frequency responses of practical filters are only approximations of the indicator functions. In particular, for small values of ϵ and δ, we want our filters to satisfy

$$\max_{\boldsymbol{\omega}\notin\partial\mathcal{X}+B(0,\delta)} |X(e^{j\boldsymbol{\omega}}) - I_{\mathcal{X}}(\boldsymbol{\omega})| \leq \epsilon, \tag{1}$$

where $\partial\mathcal{X}$ is the set of boundary points of the passband support $\mathcal{X}$, and $B(0,\delta) \stackrel{\text{def}}{=} \{\boldsymbol{\omega} : \|\boldsymbol{\omega}\| \leq \delta\}$ is the d-D ball of radius δ. Note that $\partial\mathcal{X} + B(0,\delta)$ is the transition band of the frequency response. Furthermore, we denote

$$\mathcal{R}(\mathcal{X},\epsilon,\delta) \stackrel{\text{def}}{=} \left\{ X(e^{j\boldsymbol{\omega}}) : \max_{\boldsymbol{\omega}\notin\partial\mathcal{X}+B(0,\delta)} |X(e^{j\boldsymbol{\omega}}) - I_{\mathcal{X}}(\boldsymbol{\omega})| \leq \epsilon \right\} \tag{2}$$

to be the set of all filter responses for which condition (1) holds.

2.2. The Passband Support of Hourglass Filter Banks

Definition 1 *The d-D ($d \geq 2$) nonsubsampled hourglass filter bank consists of d analysis filters $\{H_i(e^{j\boldsymbol{\omega}})\}_{i=1}^d$ and d synthesis filters $\{G_i(e^{j\boldsymbol{\omega}})\}_{i=1}^d$. The idealized passband supports $\mathcal{H}_i$ and $\mathcal{G}_i$ of the i-th analysis/synthesis filter pair, $H_i(e^{j\boldsymbol{\omega}})$ and $G_i(e^{j\boldsymbol{\omega}})$, are*

$$\mathcal{H}_i = \mathcal{G}_i = \{\boldsymbol{\omega} \in (-\pi,\pi]^d : |\omega_i| \geq \max_{j\neq i} |\omega_j|\} + 2\pi\mathbb{Z}^d. \tag{3}$$

Note that $2\pi\mathbb{Z}^d \stackrel{\text{def}}{=} \{2\pi\boldsymbol{n} : \boldsymbol{n} \in \mathbb{Z}^d\}$ represents the 2π periodicity of frequency responses. Since the analysis and synthesis filters have the same passband supports, we will concentrate on the analysis filters in the following discussions.

In the 2-D and 3-D cases, we can easily verify that the definition in (3) indeed specifies the hourglass-shaped passband supports as shown in Figure 2 and Figure 3, respectively. In the general d-D case, the geometric meaning of the defined filter supports can be interpreted as follows. For any frequency point $\boldsymbol{\omega} \in (-\pi,\pi]^d$, its minimum distance (as obtained by orthogonal projection) to the i-th frequency axis is $\sqrt{\|\boldsymbol{\omega}\|^2 - |\omega_i|^2}$. It then follows from (3) that the i-th filter $H_i(e^{j\boldsymbol{\omega}})$ only selects frequencies that are closer to the i-th frequency axis than to any other axis.

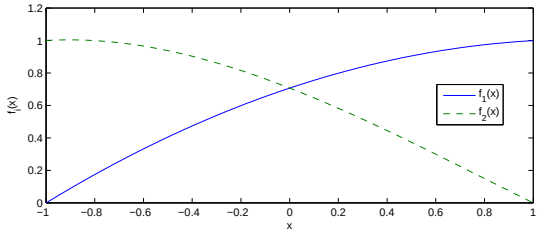

Fig. 4. Examples of 1-D prototype polynomials used in the transformation of variables.

The following result plays an important role in our proposed filter bank design discussed in the next section.

Lemma 1 *Let $\Lambda_d = \{1, 2, \ldots, d\}$ be the set of all indices and $\Lambda \subset \Lambda_d$ be one of its non-empty subsets. We have*

$$\bigcup_{i\in\Lambda} \mathcal{H}_i = \{\boldsymbol{\omega} \in (-\pi,\pi]^d : \max_{i\in\Lambda} |\omega_i| \geq \max_{j\in\,\Lambda_d\setminus\Lambda} |\omega_j|\} + 2\pi\mathbb{Z}^d. \tag{4}$$

As a special case of Lemma 1, we can choose the subset Λ to be equal to Λ_d. It then follows from Lemma 1 that $\bigcup_{i=1}^d \mathcal{H}_i = (-\pi,\pi]^d + 2\pi\mathbb{Z}^d = \mathbb{R}^d$, i.e., the d different hourglass supports cover the entire d-D frequency spectrum. On the other hand, it is clear from the definition that any two different supports $\mathcal{H}_i$ and $\mathcal{H}_j$ have disjoint interiors, i.e., they only intersect on the boundaries. Hence, we can verify that the passband supports defined in (3) indeed form a partition of the d-D frequency spectrum.

3. FILTER BANK DESIGN

In this section, we deal with the filter design of the multidimensional nonsubsampled hourglass filter banks. The goal is to find a set of FIR filters $\{h_i[\boldsymbol{n}]\}_{i=1}^d$ and $\{g_i[\boldsymbol{n}]\}_{i=1}^d$, such that their frequency responses are good approximations of the ideal hourglass filters as defined in (3), and that the perfect reconstruction condition is satisfied, i.e.,

$$\sum_{i=1}^{d} H_i(e^{j\boldsymbol{\omega}}) \cdot G_i(e^{j\boldsymbol{\omega}}) = 1. \tag{5}$$

3.1. Transformation of Variables

A common approach to the design of nonseparable multidimensional filters is based on the transformation of variables, also known as the (generalized) McClellan transform [9, 5]. In the two channel case, the basic idea of this approach can be explained as follows:

First, we find four 1-D polynomials $f_1(x), f_2(x), e_1(x)$, and $e_2(x)$ satisfying the Bezout's Identity:

$$f_1(x) \cdot e_1(x) + f_2(x) \cdot e_2(x) = 1. \tag{6}$$

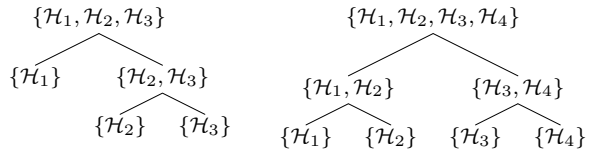

(a) The 3-D case (b) The 4-D case

Fig. 5. Construction of the multi-channel hourglass filter banks through a cascade of two-channel filter banks.

Meanwhile, we choose the polynomials so that $f_i(x) \approx e_i(x)$ for $i = 1, 2$, and that $f_1(1) = e_1(1) = f_2(-1) = e_2(-1) = 1$ and $f_1(-1) = e_1(-1) = f_2(1) = e_2(1) = 0$. The details of how to find these polynomials will be given in Section 4. Here, we just show in Figure 4 an example of the shape of these polynomials.

Let the mapping kernel $K(e^{j\boldsymbol{\omega}})$ be the Fourier transform of some multidimensional zero-phase FIR filter. Now the key step is to substitute the variable x in the polynomials with $K(e^{j\boldsymbol{\omega}})$ and define the analysis and synthesis filters as

$$F_i(e^{j\boldsymbol{\omega}}) = f_i\left(K(e^{j\boldsymbol{\omega}})\right) \text{ and } E_i(e^{j\boldsymbol{\omega}}) = e_i\left(K(e^{j\boldsymbol{\omega}})\right), \tag{7}$$

for $i = 1, 2$.

Several nice properties come from this transformation of variables. First, the perfect reconstruction condition in (5) (for $d = 2$) is satisfied with arbitrary choices of $K(e^{j\boldsymbol{\omega}})$. Meanwhile, same as the kernel $K(e^{j\boldsymbol{\omega}})$, the resulting multidimensional filters are still FIR, and have zero phase.

To control frequency responses, we can design the mapping kernel such that $K(e^{j\boldsymbol{\omega}}) \approx 2I_{\mathcal{K}}(\boldsymbol{\omega}) - 1$, where $\mathcal{K}$ is the desired passband support. It can be easily verified that $F_1(e^{j\boldsymbol{\omega}}) \approx E_1(e^{j\boldsymbol{\omega}}) \approx I_{\mathcal{K}}$ and $F_2(e^{j\boldsymbol{\omega}}) \approx E_2(e^{j\boldsymbol{\omega}}) \approx I_{\mathcal{K}^C}$, i.e., the two channels of the filter bank decompose the frequency spectrum into two parts, with the passband supports being $\mathcal{K}$ and its complement $\mathcal{K}^C$ respectively.

3.2. Extension to the Multi-Channel Case

The nonsubsampled hourglass filter banks discussed in this paper have d channels in the d-D case. To extend the transformation of variables technique to the general multi-channel case, we propose to use a cascade of two-channel filter banks.

The idea can be explained by the tree graph in Figure 5(a) for the 3-D case. The root of the tree is the entire 3-D spectrum, or equivalently the union of all three hourglass supports, denoted as $\{\mathcal{H}_1, \mathcal{H}_2, \mathcal{H}_3\}$. At the first level, we use a two channel mapped filter bank (with a kernel $K_1(e^{j\boldsymbol{\omega}})$) to divide the spectrum into two parts: $\{\mathcal{H}_1\}$ and $\{\mathcal{H}_2, \mathcal{H}_3\}$. Leaving the first node alone, we then attach another two-channel mapped filter bank (with a different kernel $K_2(e^{j\boldsymbol{\omega}})$) to further divide $\{\mathcal{H}_2, \mathcal{H}_3\}$ into $\{\mathcal{H}_2\}$ and $\{\mathcal{H}_3\}$.

Assume the polynomials used in the analysis part of the mapped filter banks are $f_1(x)$ and $f_2(x)$, then the resulting analysis filters are

$$\begin{aligned} H_1(e^{j\boldsymbol{\omega}}) &= f_1(K_1(e^{j\boldsymbol{\omega}})), \\ H_2(e^{j\boldsymbol{\omega}}) &= f_2(K_1(e^{j\boldsymbol{\omega}})) \cdot f_1(K_2(e^{j\boldsymbol{\omega}})), \\ H_3(e^{j\boldsymbol{\omega}}) &= f_2(K_1(e^{j\boldsymbol{\omega}})) \cdot f_2(K_2(e^{j\boldsymbol{\omega}})), \end{aligned}$$

and the synthesis filters take similar forms.

Note that this strategy can be easily generalized to arbitrary d-D cases. For example, we show in Figure 5(b) the cascading structure for the 4-D hourglass filter bank.

Since each two-channel mapped filter bank achieves perfect reconstruction with zero-phase FIR filters, the resulting d-channel filter banks also have perfect reconstruction with zero-phase FIR filters. The remaining task is to specify the kernels $K_i(e^{j\boldsymbol{\omega}})$ so that the resulting filters achieve the desired passband supports.

3.3. Conditions on the Mapping Kernels

At any node in a cascading tree (such as the one in Figure 5(b)), the equivalent filter $F(e^{j\boldsymbol{\omega}})$ at that node is obtained as the product of all filters along the path from the root to that node. Now suppose $F(e^{j\boldsymbol{\omega}})$ approximates the ideal indicator function on the passband support

$$\mathcal{F} = \bigcup_{i \in \Lambda} \mathcal{H}_i, \tag{8}$$

where Λ is a nonempty subset of $\Lambda_d = \{1, 2, \ldots, d\}$. We subsequently decompose $F(e^{j\boldsymbol{\omega}})$ by a two-channel mapped filter bank with a mapping kernel $K(e^{j\boldsymbol{\omega}})$, and generate two equivalent filters at the next level as

$$F(e^{j\boldsymbol{\omega}}) \cdot F_1(e^{j\boldsymbol{\omega}}) \quad \text{and} \quad F(e^{j\boldsymbol{\omega}}) \cdot F_2(e^{j\boldsymbol{\omega}}),$$

where F_1 and F_2 are the component filters of the mapped filter bank as defined in (7). We want to study the conditions on the mapping kernel $K(e^{j\boldsymbol{\omega}})$ (or equivalently on its passband support $\mathcal{K}$) so that the two resulting equivalent filters have ideal passband supports

$$\mathcal{F}_1 = \bigcup_{i \in \Lambda_1} \mathcal{H}_i \quad \text{and} \quad \mathcal{F}_2 = \bigcup_{i \in \Lambda \setminus \Lambda_1} \mathcal{H}_i, \tag{9}$$

where Λ_1 is a non-empty and proper subset of I.

Moreover, the design should allow the two resulting filters $F_1(e^{j\boldsymbol{\omega}})$ and $F_2(e^{j\boldsymbol{\omega}})$ to be arbitrarily close to the ideal indicator functions $I_{\mathcal{F}_1}$ and $I_{\mathcal{F}_2}$, provided that the filters $F(e^{j\boldsymbol{\omega}})$, $F_1(e^{j\boldsymbol{\omega}})$ and $F_2(e^{j\boldsymbol{\omega}})$ we use have good frequency responses themselves. All these requirements can be formalized as follows:

Condition 1 *For any given $\epsilon, \delta > 0$, there exist $\epsilon_1, \delta_1 > 0$ such that for any $F(e^{j\boldsymbol{\omega}}) \in \mathcal{R}(\mathcal{F}, \epsilon_1, \delta_1)$, $F_1(e^{j\boldsymbol{\omega}}) \in \mathcal{R}(\mathcal{K}, \epsilon_1, \delta_1)$, and $F_2(e^{j\boldsymbol{\omega}}) \in \mathcal{R}(\mathcal{K}^C, \epsilon_1, \delta_1)$, we have*

$$F(e^{j\boldsymbol{\omega}}) \cdot F_1(e^{j\boldsymbol{\omega}}) \in \mathcal{R}(\mathcal{F}_1, \epsilon, \delta),$$

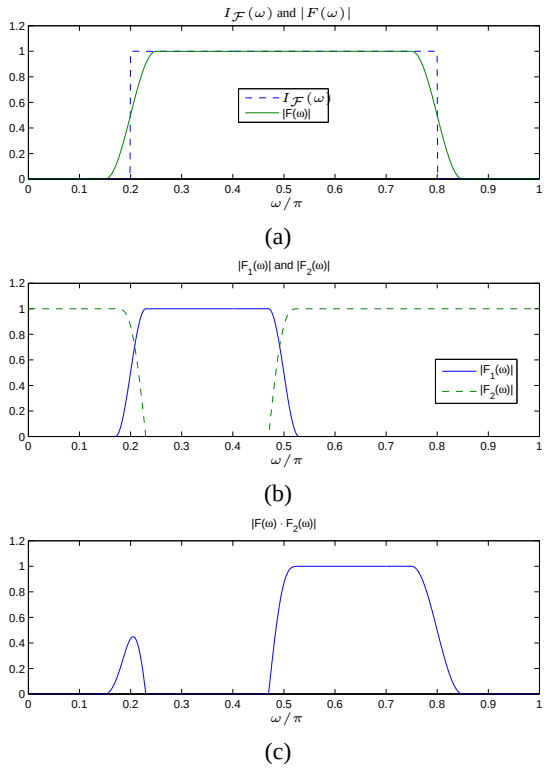

Fig. 6. Illustration of problems when the kernel support $\mathcal{K}$ is not chosen appropriately.

and

$$F(e^{j\boldsymbol{\omega}}) \cdot F_2(e^{j\boldsymbol{\omega}}) \in \mathcal{R}(\mathcal{F}_2, \epsilon, \delta),$$

where $\mathcal{F}$, $\mathcal{F}_1$, and $\mathcal{F}_2$ are the passband supports defined in (8) *and* (9)*, respectively.*

Proposition 1 *Condition 1 holds if and only if the ideal passband support $\mathcal{K}$ of the mapping kernel satisfies*

$$\mathcal{F} \cap \mathcal{K} = \mathcal{F}_1, \tag{10}$$

and

$$\partial\mathcal{F} \cap \partial\mathcal{K} \subset \partial\mathcal{F}_1 \cap \partial\mathcal{F}_2. \tag{11}$$

Intuitively, condition (10) implies that $\mathcal{K}$ "cuts" $\mathcal{F}_1$ out of $\mathcal{F}$. Furthermore, condition (11) requires that the "cut" should only happen at the location where the boundaries of $\mathcal{F}_1$ and $\mathcal{F}_2$ intersect. The purpose of condition (11) is to ensure that we can still get good frequency responses when the component filters are nonideal.

We give a simple illustration for this in Figure 6. Let $F(e^{j\omega})$ (shown in solid lines in Figure 6(a)) be a 1-D filter approximating the ideal indicator function $I_{[0.2\pi,0.8\pi]}$ (shown in dashed lines). We want to use a two-channel mapped filter bank with kernel $K(e^{j\omega})$ to decompose the original passband into $[0.2\pi, 0.5\pi]$ and $[0.5\pi, 0.8\pi]$. Suppose the passband support of $K(e^{j\omega})$ is chosen to be $\mathcal{K} = [0.2\pi, 0.5\pi]$, which satisfies (10) but not (11). In Figure 6(b), we plot the two component filters $F_1(e^{j\omega})$ and $F_2(e^{j\omega})$ resulting from this mapping kernel. Again, they are only approximations to the ideal filters. Figure 6(c) shows one of the equivalent filters $F(e^{j\omega}) \cdot F_2(e^{j\omega})$. Although most of its subband energy is concentrated on $[0.5\pi, 0.8\pi]$, there is a large "bump" at 0.2π, which is exactly the location where condition (11) fails. Note that we can reduce the width of the "bump" by employing sharper filters. However, there is no guarantee that the magnitude of the "bump" can also be reduced. On the other hand, if we choose the kernel support to be $\mathcal{K} = [0, 0.5\pi]$, which satisfies both conditions in Proposition 1, then the resulting filter responses will not contain any undesirable "bump".

The next result gives a concrete construction of a suitable kernel, which has the simplest passband shape and hence can be realized by the simplest filters.

Proposition 2 *The following passband support*

$$\mathcal{K}_o = \{\boldsymbol{\omega} \in (-\pi, \pi]^d : \max_{i \in \Lambda_1} |\omega_i| \geq \max_{j \in \Lambda \setminus \Lambda_1} |\omega_j|\} + 2\pi\mathbb{Z}^d$$

satisfies the two conditions (10) *and* (11) *in Proposition 1. Moreover, among all passband supports $\mathcal{K}$ satisfying* (10) *and* (11)*, the support $\mathcal{K}_o$ is the simplest one in the sense that $\mathcal{K}_o$ involves the least number of frequency variables and has the smallest number of boundary facets.*

4. DESIGN EXAMPLE

In this section, we apply the proposed filter bank design technique to the 3-D case. As shown in Figure 5(a), we will need to design two mapped filter banks with kernels $K_1(e^{j\boldsymbol{\omega}})$ and $K_2(e^{j\boldsymbol{\omega}})$.

4.1. Polynomials in the Mapped Filter Banks

In our design, we have chosen the polynomials in the mapped filter banks to be

$$\begin{aligned} f_1(x) &= 0.5(x+1)\left(\sqrt{2} + (1-\sqrt{2})x\right), \\ f_2(x) &= 0.5(1-x)\left(\sqrt{2} - (4-3\sqrt{2})x + (2\sqrt{2}-3)x^2\right), \end{aligned}$$

and $e_1(x) = f_2(-x)$, $e_2(x) = f_1(-x)$.

It can be easily verified that these polynomials satisfy the Bezout's Identity in (6). A nice thing about these polynomials is that $f_i(x)$ (at the analysis side) and $e_i(x)$ (at the synthesis side) are very close to each other in shape, and hence the resulting filter banks will be approximately self-inverting, i.e., form a tight frame.

4.2. Mapping Kernels Using FIR Filters

We know from Proposition 2 that the passband supports of the two mapping kernels should be

$$\begin{aligned} \mathcal{K}_1 &= \{\boldsymbol{\omega} \in (-\pi, \pi]^3 : |\omega_1| \geq \max_{j=2,3} |\omega_j|\} + 2\pi\mathbb{Z}^3, \\ \mathcal{K}_2 &= \{\boldsymbol{\omega} \in (-\pi, \pi]^3 : |\omega_2| \geq |\omega_3|\} + 2\pi\mathbb{Z}^3. \end{aligned}$$

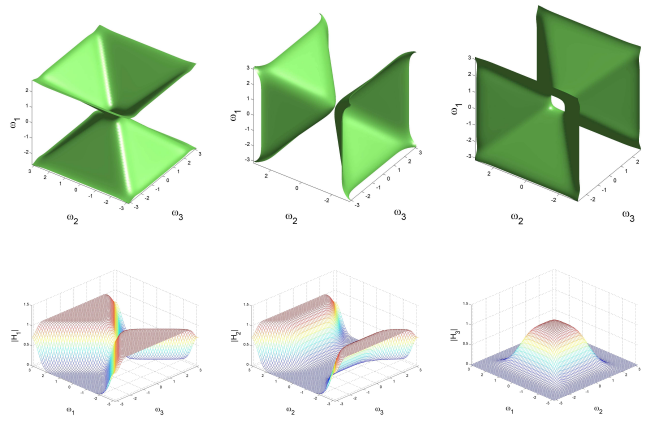

Fig. 7. Top row (from left to right): the iso-surfaces of three hourglass filters $H_1(e^{j\boldsymbol{\omega}})$, $H_2(e^{j\boldsymbol{\omega}})$, and $H_3(e^{j\boldsymbol{\omega}})$. Bottom row (from left to right): 2-D slices $H_1(e^{j(\omega_1,0,\omega_3)})$, $H_2(e^{j(\pi/2,\omega_2,\omega_3)})$, and $H_3(e^{j(\omega_1,\omega_2,\pi/3)})$.

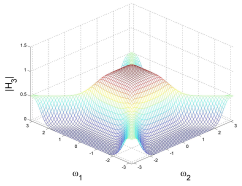

Fig. 8. The frequency response (2-D slice $H_3(e^{j(\omega_1,\omega_2,\pi/3)})$) of a 3-D filter designed by using an incorrect mapping kernel.

There are several ways to find FIR filters approximating these passband supports. In our design, we have chosen to use the multivariate Bernstein polynomial [10, 11], for its excellent approximation ability. Due to space limitations, we refer to [10, 11] for details of the design.

4.3. Filter Frequency Responses

In Figure 7 we show the frequency responses of the designed 3-D hourglass filters. Only the analysis filters are shown and the synthesis filters are very similar.

On the top row are the iso-surfaces of the three filters, which closely resemble the ideal hourglass shapes. On the bottom row are several 2-D slices of the 3-D frequency responses. Depending on the locations of the cutting planes, the 2-D slices can have fan-shaped, trapezoid-shaped, or lowpass-shaped responses.

Finally, to emphasize the importance of choosing the correct kernel passband support according to Propositions 1 and 2, we show in Figure 8 a 2-D slice of the resulting 3-D filter when we choose the second kernel to be

$$\mathcal{K}_2' = \mathcal{H}_2 = \{\boldsymbol{\omega} \in (-\pi,\pi]^3 : |\omega_2| \geq \max_{j=1,3} |\omega_j|\} + 2\pi\mathbb{Z}^3.$$

Note that this passband support only satisfies condition (10) in Proposition 1. For the same reason as we explained for the 1-D case in Figure 6, there are lots of aliasing components outside of the desired lowpass-shaped passband. This is in sharp contrast to the corresponding filter shown in Figure 7.

5. CONCLUSIONS

In this paper, we studied the multidimensional nonsubsampled hourglass filter banks. After analyzing the geometry of multidimensional hourglass-shaped passband supports, we proposed a novel design for these filter banks in arbitrary dimensions, featuring perfect reconstruction and FIR filters. We discussed necessary and sufficient conditions for the resulting filters to have good frequency responses, and provided an optimal solution that satisfies these conditions with simplest filters.

6. REFERENCES

[1] R. H. Bamberger and M. J. T. Smith, "A filter bank for the directional decomposition of images: theory and design," *IEEE Trans. Signal Proc.*, vol. 40, no. 4, pp. 882–893, April 1992.

[2] Y. Lu and M. N. Do, "Multidimensional directional filter banks and surfacelets," *IEEE Trans. Image Proc.*, in press.

[3] S. Park, *New Directional Filter Banks and Their Applications in Image Processing*, Ph.D. thesis, Georgia Institute of Technology, 1999.

[4] L. T. Bruton, "Three-dimensional cone filter banks," *IEEE Trans. Circ. and Syst., Part I Fundamental Theory and Applications*, vol. 50, no. 2, pp. 208–216, February 2003.

[5] D. B. H. Tay and N. Kingsbury, "Flexible design of multidimensional perfect reconstruction FIR 2-band filters using transformations of variables," *IEEE Trans. Image Proc.*, vol. 2, pp. 466–480, 1993.

[6] S.-M. Phoong, C. W. Kim, P. P. Vaidyanathan, and R. Ansari, "A new class of two-channel biorthogonal filter banks and wavelet bases," *IEEE Trans. Signal Proc.*, vol. 43, no. 3, pp. 649–665, Mar. 1995.

[7] K. S. C. Pun and T. Q. Nguyen, "A novel and efficient design of multidimensional PR two-channel filter banks with hourglass-shaped passband support," *IEEE Signal Proc. Letters*, vol. 11, no. 3, March 2004.

[8] A. L. Cunha, J. Zhou, and M. N. Do, "The nonsubsampled contourlet transform: theory, design, and applications," *IEEE Trans. Image Proc.*, 2006, to appear.

[9] J. H. McClellan and D. S.K. Chan, "A 2-D FIR filter structure derived from the Chebyshev recursion," *IEEE Trans. Circ. and Syst.*, vol. CAS-24, no. 7, pp. 372–378, July 1977.

[10] T. Cooklev, T. Yoshida, and A. Nishihara, "Maximally flat half-band diamond-shaped FIR filters using the Bernstein polynomial," *IEEE Trans. Circ. and Syst. II*, vol. 40, no. 11, pp. 749–751, November 1993.

[11] D. B. H. Tay, "Parametric Bernstein polynomial for least squares design of 3-D wavelet filter banks," *IEEE Trans. Circ. and Syst. I*, vol. 49, no. 6, pp. 887–891, June 2002.